Environmental Science and Pollution Research
https://doi.org/10.1007/s11356-021-12842-9

RESEARCH ARTICLE

Soil and ambient air mercury as an indicator of coal-fired power plant emissions: a case study in North China

Zhonggen Li[1,2] · Xufeng Chen[3] · Wenli Liu[3] · Taishan Li[4] · Guangle Qiu[2] · Haiyu Yan[2] · Mingmeng Wang[5,2] · Ji Chen[2] · Guangyi Sun[2] · Qingfeng Wang[1] · Xinbin Feng[2]

Received: 30 March 2020 / Accepted: 3 February 2021

Abstract

Coal-fired power plants (CFPPs) are an important anthropogenic mercury (Hg) source in China, and it is crucial to understand the environmental impacts of this detrimental element emitted from this source. In the present study, field experiments were conducted for measuring Hg in ambient atmosphere and upland agricultural soils within a radius of 10 km surrounding a large scale coal-fired power plant (1550 MW) in Tangshan, Hebei province. Short-term (20 min) average of gaseous elemental mercury (GEM or Hg^0) in ambient air varying from 1.5 to 9.0 ng/m^3 and total Hg (THg) in surface agricultural soil (0–20 cm) varying from 9.2 to 43.5 μg/kg at different sites were observed. THg in two soil cores decreased with depth, with concentrations being 2–2.5 times higher in the surface layer than that in the deep layer (50–60 cm), indicating the possibility of the atmospheric input of Hg. Based on the information of the total atmospheric Hg emission since this CFPP's operation in 1970s and the increased THg in nearby soils, it was estimated that about 3.9% discharged Hg has accumulated in the nearby agricultural soils. The low retention rate of the total emitted Hg by soils is a result of high proportion of Hg^0 (79.5%) in stack gas emission and potential loss of Hg from soil surface reemission. The positive shifting (~ 0.5‰) of Hg isotopic signature (δ^{202}Hg) from deep soil to surface soil reflected Hg deposition from nearby CFPP emissions that are featured with much heavier Hg isotopic signatures inherited from feed coal (δ^{202}Hg: –0.50‰) and different combustion products (δ^{202}Hg: –0.95 to 3.71‰) compared with that in deep soil layer (δ^{202}Hg: ca –1.50‰). Overall, this study demonstrated that this CFPP has a slight but distinguishable effect on the elevation of ambient GEM and agricultural soil THg in the local environment.

Keywords Mercury · Coal-fired power plants · Atmospheric emissions · Environmental impacts · Mercury isotopic signatures

Responsible Editor: Severine Le Faucheur

✉ Zhonggen Li
lizhonggencn@126.com

✉ Xinbin Feng
fengxinbin@mail.gyig.ac.cn

[1] School of Resources and Environment, Zunyi Normal College, Zunyi 563006, China

[2] State Key Laboratory of Environmental Geochemistry, Institute of Geochemistry, Chinese Academy of Sciences, Guiyang 550081, China

[3] Tangshan Environmental Monitoring Center of Hebei Province, Tangshan 063000, China

[4] Tangshan Institute of Environmental Protection, Tangshan 063000, China

[5] College of Environmental Science and Engineering, Taiyuan University of Technology, Taiyuan 030024, China

Introduction

Mercury (Hg) is a highly toxic metal that can migrate in environmental media and bioaccumulate in food chain and thus can pose adverse effects on ecological systems and human health (Lindqvist et al. 1991; Driscoll et al. 2013; Gutiérrez-Mosquera et al. 2018; Wright et al. 2018; Gustin et al. 2020). Large quantities of Hg have been released into the environment as a result of human activities since the industrial revolution, and Hg in atmosphere is subject to large-scale circulation, as well as wet/dry depositions (Lindqvist et al. 1991; Mason et al. 1994; Streets et al. 2011; Cheng et al. 2020). Coal combustion has become a vital atmospheric Hg source in the past half century on the global scale (U.S. EPA 1997; UNEP 2002; Streets et al. 2011; AMAP/UNEP 2008; UNEP 2019), and Hg emissions from this source accounted for 1/2–2/3 of the global total anthropogenic emissions in the 1990s and early 2000s (Pacyna and Pacyna 2002; UNEP 2002;

Published online: 26 February 2021

AMAP/UNEP 2008). The total accumulated Hg released into the air, land, and water from this source sector since the 1850s has reached 38.0 Gg (10^9 g, 1000 Mg or 1000 tonnes) (Streets et al. 2018). Proper management and control of Hg emissions from this source sector, as well as understanding the impacts of Hg on the environment, are a major issue for this detrimental element (UNEP 2019). In this regard, coal-fired power plants (CFPPs), especially the large scale ones, deserve more attention (Antonio et al. 2016; Zhang et al. 2015).

With a rich coal and lean oil energy structure, as well as the rapidly increasing economy since late 1970s, China became the world's largest coal user since 1989 and now consumed about half of the world's total coal output each year (Dai and Finkelman 2018). As a result, atmospheric Hg emissions from coal combustion in China has totaled over 5000 tonnes in the period of 1978–2010 (Wang et al. 2000; Zhang et al. 2015). CFPPs is the largest domestic coal user, consuming 45–50% of the national total coal production in the past two decades (Dai and Finkelman 2018). Atmospheric mercury emissions from this source were estimated to be 48–105 tonnes/yr during 1999–2017, accounting for 10.8–21.9% of the national total anthropogenic emissions (Streets et al. 2005; Zhang et al. 2015; Liu et al. 2019).

Although plenty of studies have been carried out on Hg emissions from the Chinese CFPPs (Tang et al. 2007; Wang et al. 2011a; Li et al. 2019), Hg contamination in different environmental media around Chinese CFPPs has not been adequately investigated. In addition, most of the existing studies focused on regions in South and Central China, e.g., Hunan province (Xu et al. 2017), Guizhou province (Yang et al. 2012), Anhui province (Tang et al. 2013), and Zhejiang province (Zheng et al. 2009), albeit the national coal resource and CFPPs are mainly distributed in North China (Dai and Finkelman 2018; Liu et al. 2019). A recent study investigated the soil Hg concentration in central Inner Mongolia of North China and found that the Hg concentration in topsoil (0–10 cm) increased ca. 50% compared to that of the subsoil at 20–30 cm as a result of atmospheric Hg deposition originated from dozens of CFPP emissions within hundreds of kilometers (Cheng et al. 2020). However, little is known about the impacts of Hg emission from CFPPs in the local scale (such as <50km) in North China, where important grain planting and animal husbandry areas are located.

Moreover, Hg isotope techniques have been developed rapidly in the past two decades and have been proved to be a useful tool in tracking Hg emission sources and behavior in the environment (Blum and Bergquist 2007; Sun et al. 2019a). Mercury isotopic signatures have been reported for stack emissions of CFPPs and some important Hg-bearing mineral resources like Hg ore and Zn ore (Tang et al. 2017; Wiederhold et al. 2013; Yin et al. 2016), providing critical basis for constraining the global isotopic signatures of Hg emissions (Sun et al. 2016) and tracing associated environmental impacts (Sherman et al. 2012; Huang et al. 2016). While there are some limited reports on Hg isotopic signature in different environmental media around CFPPs, such as lake sediments (Jackson and Muir 2012) and the precipitant (Sherman et al. 2012; Huang et al. 2018), there are no reports for soil yet, although it is considered as a good achieve of CFPPs emissions (Antonio et al. 2016).

Based on these above-mentioned reasons, the present study was designed to analyze the Hg concentration in upland agricultural soils and atmosphere within 10 km radius surrounding a large scale CFPPs (with a total installed capacity of 1550 MW) that has run for more than 40 years in the North China Plain (NCP). Mercury isotopic signatures in the agricultural soils, feed coal, and different coal combustion products inside the CFPP were also determined. The objectives of this study are to (1) disclose the contamination level of Hg in ambient atmosphere and agricultural soil around this CFPP, (2) evaluate the retention of Hg in local soil that is impacted by this CFPP emission, and (3) reveal the possible links of CFPP emissions and the nearby soil Hg accumulation.

Materials and methods

Study area and the CFPP

The NCP is one of the most important granaries of China and covers an area of ca. 300,000 km^2 (Gao et al. 2020); it provides about one fourth of the country's total cereal crops (Wang et al. 2016). Tangshan belongs to the northeast edge of the NCP and is a traditional coal industrial city in the region of Beijing-Tianjing-Hebei (Fig. 1). Coal mining and coal-based industries have induced a variety of environmental issues, such as environmental pollution (e.g., Hg), landscape destruction, and land subsidence (Sun et al. 2019b). The study area is surrounding a large scale CFPP located in the northeast suburb (Kaiping district) of Tangshan city, Hebei province, with a distance of about 20 km to the city center and about 170 km to Beijing in the east (Fig. 1). The CFPP has been operated since 1976 and has eight units (each 125 to 250 MW) with a total installation capacity of 1550 MW, making this CFPP the largest one in China during the 1970s to 1980s (Zheng et al. 2015). Flue gas of this CFPP was discharged into ambient atmosphere through four 180 m stacks with every two units sharing one stack. A total of 17.5 tonnes of Hg was emitted from this CFPP during the past four decades (1976–2013) before the present research was conducted (Li et al. 2019). The emission ratio between gaseous elemental mercury (GEM or Hg^0), gaseous oxide mercury (GOM or Hg^{2+}), and particulate-bound mercury (PBM or Hg^p) are 79.5%:17.9%:2.6% (Li et al. 2019, Fig. S1 in Electronic Supplementary Material

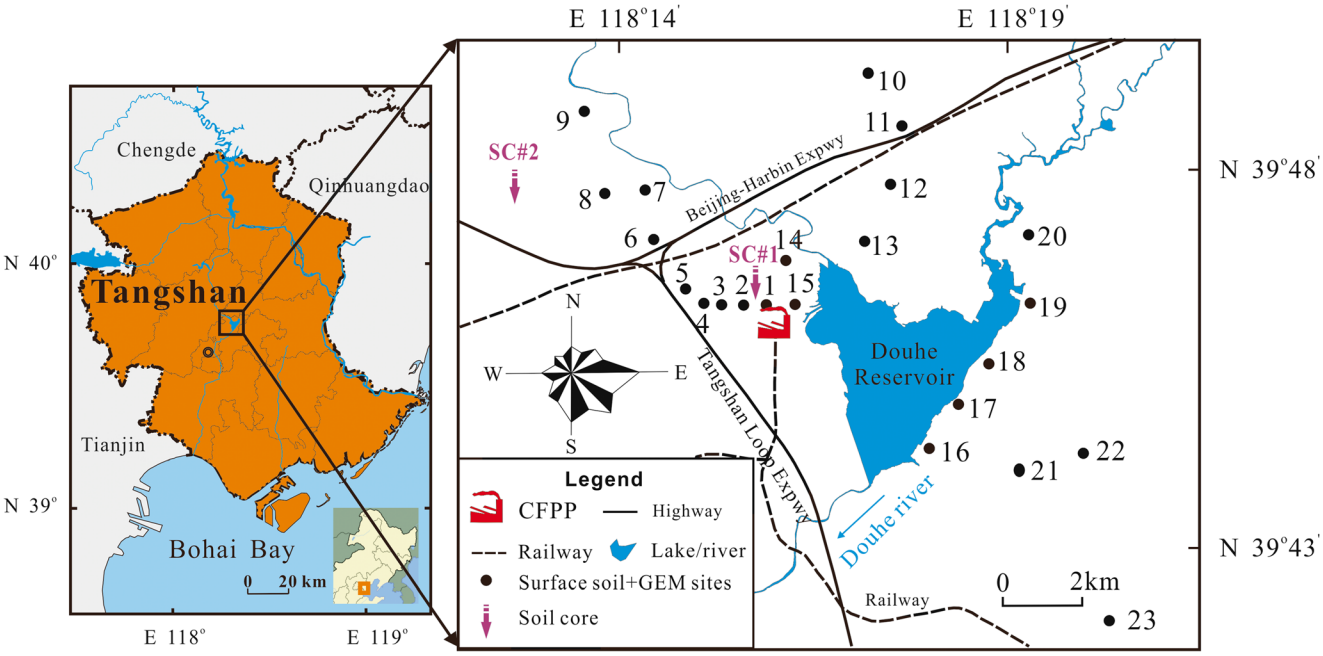

Fig. 1 Study area and the sampling sites of agricultural soil and ambient atmosphere around the CFPP

(ESM)). Most of the accumulated total Hg emissions (ca. 90%) occurred before 2008, with the highest annual level emission of ~600 kg/yr reached in 1988–2004, reduced dramatically after mid-2000s, and declined to a level of 123 kg/yr in 2013 due to the gradually improved emission control technologies, such as wet flue gas desulfurization for SO_2 and selective catalytic reduction for NOx treatment (Li et al. 2019).

The surrounding landscapes of this CFPP are agricultural land farms except a few villages and small towns scattered in the southwest direction (Fig. 1). The soils mainly consist of cinnamon and brown soil that are formed from fluvial, alluvial, and lake-marsh deposits during the Quaternary (Jiang 2006), and with a clay, silt, and sand ratio of 12%:43%:45% (Gao et al. 2020). Summer corn-winter wheat rotation system is widely applied, with corn grown during June to October and wheat from October to next June. Such corn-wheat rotation farms accounted for 86% of agricultural areas in the NCP (Gao et al. 2020). The terrain is quite flat with elevations ranging from 5 to 50 m above the sea level, except for a few dunes of about 100 m height scattered at the east and north shoreline of a reservoir in southeast direction of the CFPP.

The annual precipitation in Tangshan city is 644 mm which concentrated in July and Autumn, and the annual evaporation is 1022 mm, and the local annual average temperature is 10.6 °C. The wind direction is predominantly from the east, except in winter (December–February) when the wind is from the west and the west-north-west directions (Sun et al. 2019b).

Sample collection

Field samples were collected in August 2013. Twenty-three sampling sites (Fig. 1), all of which were on corn-wheat rotation fields, within 10 km of the CFPP, were chosen based on local wind direction, agricultural land distribution, and local industrial distribution to avoid possible human disturbance from the southwest direction of the CFPP where located dwelling and construction zones (Sun et al. 2019b). One surface soil (0–20 cm) sample at each site was obtained from a mix of five subsamples collected within 100 m^2 of the sampling site. Ambient GEM was measured at 1 m above the ground for 20 min to gain an average value at each site. In addition, two soil cores (50–60 cm depth) 6 km apart were collected with a 5-cm vertical interval (Fig.1). All soil samples were kept in the polyethylene ziplock bags, and carried back to the laboratory, where they were air-dried, ground, and passed through a 0.150-mm nylon sieve. A reference site with similar physicochemical and climatic conditions would be an idea for cross exanimation of the measured soil Hg concentration and isotopic feature, however, such an ideal reference site is difficult to locate in the NCP because of the densely distributed CFPPs in this region, including Tangshan city and Hebei province (Sun et al. 2019b; Liu et al. 2019), which could impact the regional environments hundreds of kilometers away (Cheng et al. 2020). Nevertheless, we sampled the deep soil layer to reflect the local soil background because it is least impacted by atmospheric deposition of Hg.

Within the CFPP, different solid samples, including feed coal, fly ash, gypsum, and stack flue gas samples, were also collected in the same month for the Hg isotopic analysis, as

detailed in the ESM and Fig. S2. These sampled materials represent the majority of Hg input or output of the CFPP.

Analytical methods and quality assurance

Analysis of total Hg in soils

Total mercury (THg) in soils was measured using a RA915+ Hg analyzer equipped with PYRO 915+ pyrolysis attachment by way of thermal decomposition to Hg^0 (Lumex Ltd., Russia) (Li et al. 2019). All samples were analyzed three times to gain an average value. Accuracy was assessed using the certified reference materials (CRMs) GSS-13 and GSS-8 which represent soils from North China, and the recoveries of Hg ranged from 88.2–92.3% (Table S1).

Soil pH and soil organic matter determination

pH of soil was measured with deionized water in a 2.5:1 (w/w) water/soil ratio using a pH meter (NY/T 1377- 2007), and soil organic matter (SOM) content was determined by the potassium dichromate method (NY/T 1121.6- 2006).

Measurement of ambient GEM

Ambient GEM was sampled and analyzed using a Lumex RA-915+ analyzer. The analyzer is based on differential Zeeman atomic absorption spectrometry using high frequency modulation of light polarization (ZAAS-HFM). The instrument is calibrated with an internal Hg source every 24 h and runs on an online mode with a time resolution of 30 s and a detection limit of 0.3 ng/m^3 (Wang et al. 2011b).

Detection of Hg isotopic composition

Solid samples of soil, feed coal, fly ash, and gypsum were pretreated by a double-stage tube furnace; Hg in these samples were volatilized and trapped into a 40 % (v/v) mixture solution ($2HNO_3$/1HCl, v/v) (Sun et al. 2013), and then the Hg isotopic compositions were measured by Nu Plasma II multiple-collector inductively coupled plasma mass spectrometry (MC-ICP-MS, Nu Instruments, UK) equipped with a gas/liquid phase separator (Yin et al. 2010), using $SnCl_2$ (3%) as the reducing agent to generate gaseous Hg^0 entering into a plasma exciter. Liquid samples of flue gas absorption fluid were determined directly by MC-ICP-MS. Instrumental mass bias correction was accomplished using NIST SRM 997 as an internal standard and external standard-sample bracketing with a NIST SRM 3133 Hg solution.

Mass-dependent fractionation (MDF) is reported as δ^{xxx}Hg (where xxx = 199, 200, 201, or 202, Eq 1) using the unit of per mil (‰) referenced to the NIST SRM 3133 (Blum and Bergquist 2007):

$$\delta^{xxx}\mathrm{Hg}\ (‰) = 1000 \times \left[\frac{\left({}^{xxx}\mathrm{Hg}/{}^{198}\mathrm{Hg}\right)_{\mathrm{sample}}}{\left({}^{xxx}\mathrm{Hg}/{}^{198}\mathrm{Hg}\right)_{\mathrm{NIST\ 3133}}} - 1 \right] \quad (1)$$

Mass-independent fractionation (MIF) is reported as Δ^{xxx}Hg (where xxx = 199, 200, or 201) in per mil (‰) and is calculated following equations (2) to (4):

$$\Delta^{199}\mathrm{Hg}\ (‰) = \delta^{199}\mathrm{Hg} - 0.2520 \times \delta^{202}\mathrm{Hg} \quad (2)$$

$$\Delta^{200}\mathrm{Hg}\ (‰) = \delta^{200}\mathrm{Hg} - 0.5024 \times \delta^{202}\mathrm{Hg} \quad (3)$$

$$\Delta^{201}\mathrm{Hg}\ (‰) = \delta^{201}\mathrm{Hg} - 0.7520 \times \delta^{202}\mathrm{Hg} \quad (4)$$

As for the reproducibility of Hg isotope data, certified reference materials (UM-Almadén, NIST SRM 1632d (coal) and GSS-4 (soil)) were analyzed along with the samples. The isotopic compositions of CRMs in this study were in good agreement with previously published data (Table S2).

Data processing

The commercially available statistical software package SPSS v.18 (SPSS Inc. USA) was used for the statistical analysis of the dataset obtained in the present study. In this software, one-way analysis of variance (ANOVA) and independent-samples *t* test were used for statistical significance analysis, with a probability of 0.05 or lower being considered as significant. Figures of the dataset were drawn with Origin 8.6 (Origin Lab Corporation, USA).

Results and discussion

GEM in the ambient air

Average GEM in the ambient atmosphere at 23 sites around the power plant ranged from 1.5 to 9.0 ng/m^3 with an overall average of 2.7±1.7 ng/m^3 (Table 1). The average value was over 50% higher than the regional background concentration in North China (Changbai Mt., 1.60±0.51 ng/m^3, Fu et al. 2012) and was also higher (p<0.05) than those at the background sites of North Hemisphere (1.1-1.7 ng/m^3, Ebinghaus et al. 2002; Kalinchuk et al. 2018).

The average GEM of this study was comparable to those obtained in Northern China, e.g., at one suburb site in Beijing (3.48 ng/m^3) that was affected by the local/regional emissions from CFPPs, coal-fired industrial boilers, cement plants, and iron and steel factories (L. Zhang et al. 2013), and at an agricultural site in Shandong province (3.3 ng/m^3) that was mainly affected by emissions from CFPPs (Sommar et al. 2016).

Table 1 Comparison of ambient GEM around different CFPPs in the world

Locations	Distance to CFPP (km)	Range of GEM (ng/m^3)	Mean± standard deviation of GEM (ng/m^3)	Reference
Hebei, China	<10	1.5–9.0	2.7±1.7	This study
Hunan, China	<10	21–39	28±4.4	Xu et al. (2017)
Zhejiang, China	<5	4.3–12.4	7.0±2.1	Zheng et al. (2009)
Two CFPPs in Shanghai, China	<3	9.7–22.9	11.6, 17.9	Wang et al. (2011b)
Guizhou, China	<5	2–17	n.a.	Jiang et al. (2007)
Alberta, Canada	5–10	0.7–9.5	1.57	Mazur et al. (2009)
Two CFPPs in Southeast USA	7–25	n.a.	1.5–1.7	Edgerton et al. (2006)
NY, USA	5–12	n.a.	1.8±0.3	Wang et al. (2013b)
Colorado, USA	<1	1.0–7.8*	1.6±0.3*	Gratz et al. (2019)

n.a., not available; *total gaseous mercury (*TGM*)

Thus, GEM in the whole NCP has been elevated to some extent due to the extensively distributed anthropogenic emissions.

Compared with other sites around CFPPs worldwide (Table 1), the results of this study were much lower than those around some CFPPs in southern China (average values of 7.0–28 ng/m^3) (Xu et al. 2017; Zheng et al. 2009; Wang et al. 2011b; Jiang et al. 2007), but were evidently higher than those at several sites in western Canada and Midwest USA (average values of 1.5-1.8 ng/m^3) (Mazur et al. 2009; Edgerton et al. 2006; Wang et al. 2013b; Gratz et al. 2019). This discrepancy might be caused by several reasons, including the Hg emission intensity of each CFPP, regional atmospheric background, and meteorological conditions (Zhang et al. 2015; Zheng et al. 2009; Jiang et al. 2007). Compared with ambient GEM at sites around (<10 km), other anthropogenic sources, such as Zn smelter (average value of 19.5 ng/m^3, Wu et al. 2014), closed chlor-alkali plant (average value of 35.4 ng/m^3, Zhu et al. 2018), closed polyvinyl chloride (PVC) workshop (average value of 188 ng/m^3, Zhu et al. 2018), and artisanal Hg smelting areas (average value of 40 μg/m^3, Li et al. 2008), GEM around the CFPP in the present study is actually much low. Furthermore, GEM around this CFPP is below the limit (50 ng/m^3) of national standard for ambient air quality of China (GB 3095– 2012).

The ambient GEM concentrations sampled at the 23 sites showed no obvious spatial trend (p>0.05) with distance to the CFPP (Fig. 2a), likely because of the high stack height (Li et al. 2019; Zhang et al. 2015) and/or the fugitive emissions from this CFPP (Wu et al. 2014; Chen et al. 2009); the latter includes the wastewater treatment, air-surface emission from material piles, and the raw material grounding process. Previous studies based on dispersion modeling results or field monitoring data indicated that CFPP emissions could increase ground-level GEM by 0.2–3.0 ng/m^3 within 3–12 km distance of CFPPs (Wang et al. 2011b; Mazur et al. 2009; Wang et al. 2013b), which was consistent with our GEM observation at near ground-level (1 m height).

Physicochemical properties and total Hg in surface soils

The descriptive statistics of soil organic matter (SOM) and pH in surface agricultural soils are listed in Table 2. SOM in the study area is low, ranged from 1.0 to 3.75% and averaged at 1.52±0.57%, which is comparable to those in the soils (1.67 ±0.75%) in Fengrun district of Tangshan city 30 km southwest of the CFPP (Jiang 2006) and soils (1.42±0.64%) from a larger area in Tangshan city that covers the downtown, Fengnan district, Kaiping district, and Guye district (Sun et al. 2019b). This implies that the influence of CFPP emissions on the local SOM was not evident (Fig. 2b). Soil pH in this study showed a medium to weak alkaline property (range 5.88–8.23; average: 7.40±0.73), which is similar to those of soils from a larger area of Tangshan city (range: 5.16–9.08; average: 7.58±0.89) (Sun et al. 2019b). The majority of acidic gases (e.g., SO_2) was released into the surrounding atmosphere from CFPPs when flue gas desulfurization devices were not widely installed in Chinese CFPPs before mid-2000s, and soil acidification was found to be more serious (pH=ca. 4) around some CFPPs in southern China that was fed with high sulfur (2–4%) coal (Mou and Tang 1992). Although the CFPP in this study consumed coals with low sulfur content (0.52%, Li et al. 2019), the influence of stack emissions on soil pH was distinctive, as indicated by the significantly positive correlation between distance and pH (Table 4; Fig. 2c).

Total Hg in surface soil of the studied area was in the range of 9.2–43.5 μg/kg, with an average of 20.7±10.0 μg/kg. These values were comparable to those previously reported for another district (Fengnan) of Tangshan city (range 15–76 μg/kg,

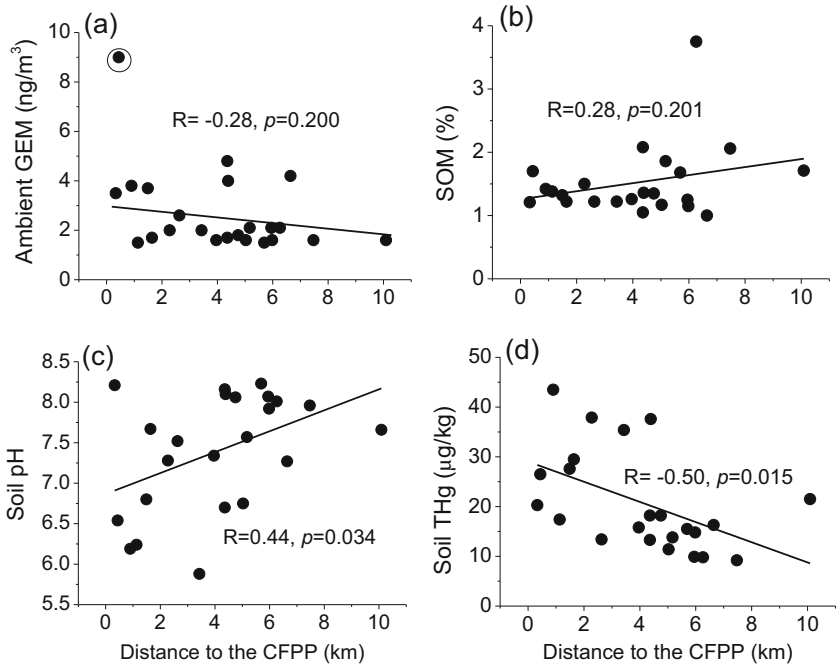

Fig. 2 Ambient GEM (**a**), and different parameters of SOM (**b**), pH (**c**), and THg (**d**) in surface agricultural soil with respect to distance to the studied CFPP

average: 27±10 μg/kg, Zhang 2017) that was also suffered from coal mining and coal-based industrial activities. THg in soil in this study was much lower than the risk screen value (2.4 mg/kg) for agricultural soil in China (GB 15618– 2018). Generally, soil THg concentrations presented here were comparable to many other measurements around CFPP sites worldwide, e.g., in the USA (6–55 μg/kg, Crockett and Kinnison 1979; Sullivan et al. 2005), central-east China (1–36 μg/kg, Tang et al. 2013; Liu et al. 2012), Greece (1–59 μg/kg, Martin et al. 2014), South Africa (30–100 μg/kg, Okedeyi et al. 2014), and some CFPPs in Spain and Chile (5–44 μg/kg, Antonio et al. 2016; Pérez et al. 2019) (Table 3), where all soil THg were below 100 μg/kg. However, it should also be noted that much higher values than mentioned above have also been reported frequently in China, e.g., Hunan province (68–220 μg/kg, Xu et al. 2017), Zhejiang province (45–529 μg/kg, Zheng et al. 2009), Guizhou province (92–320 μg/kg, Yang et al. 2012), Shaanxi province (197–2105 μg/kg, Yang and Wang 2008), Shanghai city (41–169 μg/kg, Lu et al. 2006), and outside China, e.g., Spain (200–1400 μg/kg, Antonio et al. 2016) and Chile (94–568 μg/kg, Pérez et al. 2019). Hg in soil is affected by many factors, such as total amount and speciation of Hg emitted from the anthropogenic/natural sources, height of the emission sources, and meteorological conditions (Zhang et al. 2015). CFPPs discharging more PBM and GOM would result in more serious Hg deposition in local soils due to their fast removal processes by dry and wet deposition (Gworek et al. 2017), as was found in Spain (Antonio et al. 2016), Czech (Navrátil et al. 2016), Chile (Pérez et al. 2019), and China (Li et al. 2017). In Chongqing city, southwest China, it was observed that soil Hg increased by 40 μg/kg during a 5-year span in the 1980s due to the local CFPP emissions (Mou and Tang 1992). Soil Hg increase is more discernible within a shorter distance (such as <15 km) to CFPPs than distance beyond, which has been confirmed by many cases (Antonio et al. 2016; Crockett and Kinnison 1979; Sullivan et al. 2005). The small fractions of GOM and PBM emitted from this CFPP (Fig. S1) might be an important reason for the light soil Hg contamination in the local environment.

Soil THg varied with the distance to the CFPP, and the significantly negative correlation between distance and THg was obtained (Table 4; Fig. 2d), this was a result of Hg and other ions in the precipitation and the deposition of escaped fly ash decreased with distance to CFPPs (Dutt et al. 2009; Antonio et al. 2016). THg in soils within 4 km distance (26.7±10.1 μg/kg) was obviously (p<0.05) higher than that of further distance (16.1±7.4 μg/kg, Fig. 2d), a phenomenon

Table 2 Physicochemical properties and THg in surface agricultural soils in this study (N=23, on air-dry basis)

Items	SOM (%)	pH	THg (μg/kg)	Distance to the CFPP (km)
Min.	1.00	5.88	9.2	0.33
Max.	3.75	8.23	43.5	10.09
Mean	1.52	7.40	20.7	4.10
S.D.	0.57	0.73	10.0	2.49
Median	1.35	7.57	17.4	4.36

SOM soil organism matter, *Min.* minimum, *Max.* maximum, *Mean* arithmetic average, *S.D.* standard deviation

Table 3 Comparison of Hg concentration in soils around CFPPs in the world

Region	Distance to source (km)	Range of THg (μg/kg)	Mean±standard deviation of THg (μg/kg)	Reference
Hebei, China	<10	9.2–43.5	20.7±10.0	This study
Anhui, China	<10	1–20	10	Tang et al. (2013)
Henan, China	<2	5.7–36.4	18.3	Liu et al. (2012)
Hunan, China	<10	68–220	130±40	Xu et al. (2017)
Zhejiang, China	<5	45–529	180±91	Zheng et al. (2009)
Shanghai, China	<2	41–169	n.a.	Lu et al. (2006)
China	<10	125–383	n.a.	Li et al. (2017)
Guizhou, China	1	92–320	178±62	Yang et al. (2012)
Shaanxi, China	<3	197–2105	692±429	Yang and Wang (2008)
NM, USA	<30	6–45	16±6.7	Crockett and Kinnison (1979)
Two CFPPs LV&H, Chile	<5	5–44	17±10; 24±17	Pérez et al. (2019)
Midwest USA	<8	11.6–55.4	27.6±6.9	Sullivan et al. (2005)
Greece	<20	1–59	9	Martin et al. (2014)
CFPP # 7, Spain	<45	30–40	n.a.	Antonio et al. (2016)
South Africa	<30	30–100	66±20	Okedeyi et al. (2014)
Two CFPPs R &V, Chile	<5	94–568	186±125; 355±158	Pérez et al. (2019)
CFPP #10–11, Spain	<45	200–1400	n.a.	Antonio et al. (2016)

n.a., not available

that is similar to previously reported in other places (Crockett and Kinnison 1979; Antonio et al. 2016). Similarly, soil pH within 4 km distance (6.97±0.75) was much lower than that of distance beyond 4 km (7.73±0.52, Fig. 2c).

Ambient GEM only has weak correlations with soil THg and pH (Table 4); this might be because GEM varied significantly in recent years due to the new technologies installed in the CFPP, while soil THg and pH reflect the long-time impacts of the CFPP.

THg in soil cores and soil retentions

Profiles of THg, SOM, and pH in two soil cores are illustrated in Fig. 3. THg in both soil cores decreased with depth, and the maximum reached to ca. 50 μg/kg. The Hg enrichment factor, which is defined as the ratio of THg in top soil to that in deep soil, was about 2–2.5 (Fig. 3a, b), indicating that Hg in soils was mainly input from the atmospheric deposition. THg in deep soil layer of 50–60 cm was at a level of 18–19 μg/kg, and in deep soil layer of 120 cm was at an even lower value of 15 μg/kg in Fengrun district, southwest Tangshan (Jiang 2006). The lowest value of deep soil Hg in NCP was at 10 μg/kg, based on measurements of 102 soil cores in this region (Rao and Wang 1987). Therefore, the value of 10 μg/kg was taken as the background level for local soils in this study. In addition, THg in the two soil cores is higher than that observed in Inner Mongolia (with average THg values of 14.9 μg/kg in 0–10 cm depth and 8.9 μg/kg in 20–30 cm depth), a neighboring province to Hebei in the north and also suffered from CFPPs emissions in the regional scale (Cheng et al. 2020). This finding indicates that soils around this CFPP suffered more Hg input that did soils in Inner Mongolia.

SOM was much enriched in the upmost 10 cm layer and decreased with soil depth in both soil cores (Fig. 3c,d). SOM in soils of wheat-corn cropping systems of North China was mainly derived from wheat (70%) and to a less extent (30%) from corn (Wang et al. 2013a). Soil pH was distinctively acidified in the surface layer than in the deep layer (Fig. 3c, d), and a value as low as ca. 5.0 was found in the surface layer versus 7.0 in the deep layer, indicating the impacts of CFPP emissions.

Table 4 Correlations of THg, SOM, and pH in surface agricultural soil and GEM in ambient atmosphere around the studied CFPP

Parameters	THg	GEM	SOM	pH	Distance
THg	1.00				
GEM	0.31	1.00			
SOM	−0.23	0.04	1.00		
pH	−0.40	−0.17	0.30	1.00	
Distance	−0.50*	−0.28	0.28	0.44*	1.00

**p< 0.01 level (2-tailed); *p< 0.05 level (2-tailed)

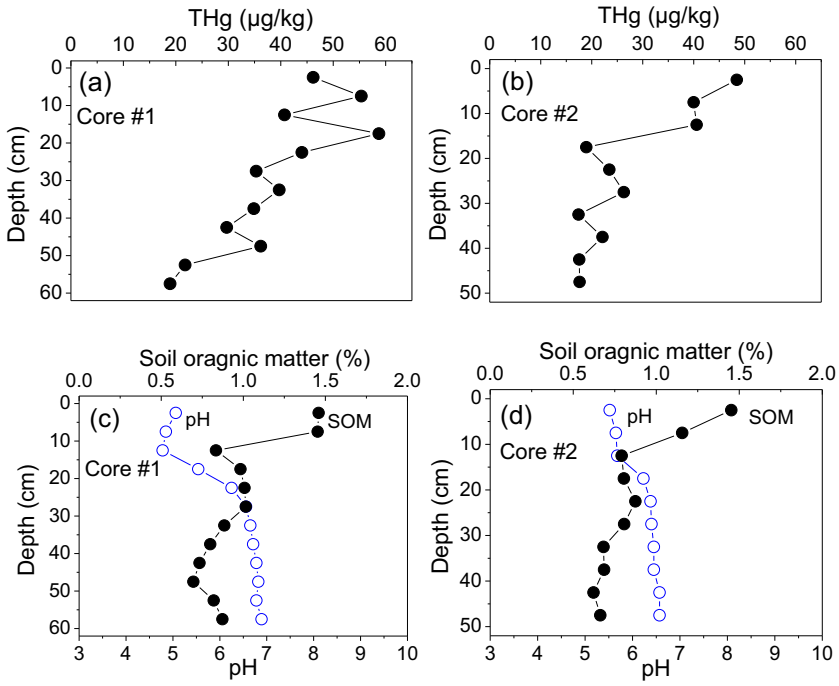

Fig. 3 Vertical distribution of THg, SOM, and pH in two soil cores

Based on the THg level in the surface soil (0–20 cm) and the soil density of 1.4 g/cm^3 (Gao et al. 2020), it was roughly estimated that about 0.69 tonnes Hg was accumulated in the surface soil within 10 km distance to the CFPP, and this amount can account for 3.9% of the total atmospheric Hg emissions from the CFPP. It was previously estimated that only a small fraction (<5%) of the total emitted Hg from CFPPs would deposit into soils within 50 km distance, and 50% GOM and <2% GEM would deposit within 480 km distance (Lohman et al. 2006; Seigneur et al. 2006), which seem to agree with our results in the present study. In addition, other reasons for the low retention of Hg in soils would be the reemission of previously deposited Hg (Eckley et al. 2015) and the leaching of soil Hg, because the ultimate soil Hg concentration is a balance of input by atmospheric deposition and the loss of Hg from soil leaching/runoff and volatilization (Wu et al. 2014). Regarding the soil Hg emission, annual soil–air Hg exchange flux of 5.46 to 7.1 ng/m^2·h (positive value representing emissions) was observed from two corn-wheat rotation croplands in Shandong province and Hebei province in the NCP (Sommar et al. 2016; Gao et al. 2020), which have similar weather and soil conditions as our study area. Applying these emission flux numbers to the area of the 10-km (in radius) circle surrounding the CFPP, soil reemissions would substantially alleviate the soil Hg accumulation by 0.56–0.72 tonnes during the past 37 years (1976–2013). As for the leaching out of soil Hg, the amount would be very limited considering that soil Hg binds strongly with soil organic matter and clays (Rydberg et al. 2010; O'Connor et al. 2019). For example, only a negligible portion of <0.2% and <0.5% was leached out by soil water in measurement study for soils from Sweden (Xu et al. 2014) and China (Yin et al. 2013), respectively, and the total soil leaching was assumed to be zero in some model estimations (Wu et al. 2014). In addition, Wang et al. (2016) found that Hg in the tillage layer (0–20 cm) of a site in the NCP was unlikely to migrate downward due to large amounts of clay minerals which adsorb Hg on clay mineral surfaces, or due to the hydrogeological conditions (i.e., reduced permeability).

It should be noted that a portion of soil Hg input is from Hg wet deposition. Annual Hg wet deposition of 8.8 μg Hg m^{-2} yr^{-1} was recorded in an agricultural observation station in Shandong province in 2013 (Sommar et al. 2016), and this value was slightly higher than the soil reemission flux intensity mentioned above. Higher dry and wet Hg deposition was anticipated in early years when Hg emissions from CFPPs were not properly curbed before the 2000s, knowing that the dry and wet Hg deposition is dominantly affected by the local emissions (Keeler et al. 2006;Zhang and Jaeglé 2013).

Hg isotopic signatures in the emission source and the receptor soils

Hg isotopic compositions in agricultural soils and CFPPs emissions are tabulated in Table S3, and MDF (δ^{202}Hg) vs IMF (Δ^{199}Hg) is plotted in Fig. 4. Possible Hg input to the terrestrial system reported in literature is also provided in Fig 4. A slightly positive shifting of δ^{202}Hg (up to 0.5‰) from the bottom soil layer (−1.54 to −1.41‰,N=2) to the surface layer (−1.12±0.09‰, 1 SD, N=7) was found in soil core #1 (Table S3 and Fig.

4). Such a shifting was likely triggered by Hg emissions from the nearby CFPP, which were featured with much heavier δ^{202}Hg signals in feed coal (−0.50±0.15‰, 1 SD, *N*=3) and the coal combustion products (−0.95 to 3.71‰), specifically, δ^{202}Hg values of −0.95 to −0.66‰ in fly ash, −0.22 to −0.13‰ in gypsum, and 0.10 to 3.71‰ of GOM and GEM in the stack gas. In addition, negative MIF was found in feed coal (Δ^{199}Hg: −0.18 to −0.12‰) and the combustion products (up to −1.13‰), while the effects of CFPP emissions on the negative shifting of soil Δ^{199}Hg signal were negligible (<0.1‰) (Fig. 4).

The Hg isotope signatures for agricultural soil, fly ash, and stack emissions obtained in the present study (Fig. 4) were different from those reported in literature, e.g., ambient PBM in Beijing (Huang et al. 2016), ambient PBM and precipitation nearby a CFPP in southeastern China (Huang et al. 2018), and precipitation nearby a CFPP in Florida, USA (Sherman et al. 2012), which is related to the differences in Hg isotopic signals in feed coals of CFPPs and APCD removal efficiencies (Sun 2019) and various Hg sources in ambient PBM and precipitation Hg. Mercury isotopic signatures in street dust of Tangshan (Sun et al. 2020) lied in between those of the surface soil and deep soil, implying that they were affected by the same source, namely, the feed coal and coal combustion from the CFPP (Sun et al. 2019b; Cui et al. 2020).

Another important source to soil Hg is the litter fall since plant leaves absorb atmospheric GEM (Zheng et al. 2016). Plant root mainly assimilates Hg from the soil but hardly transfers it to the aboveground part of the canopy (Cui et al. 2014; Niu et al. 2011), hence does not change the soil Hg pool. Corn leaf (δ^{202}Hg:-3.44±0.63‰) from Guizhou province, southwest China (Sun et al. 2019a) and the forest litters (δ^{202}Hg: −1.94 ±0.45‰) in the USA (Zheng et al. 2016) had much lighter δ^{202}Hg than did the deep soil layer (δ^{202}Hg: −1.48±0.09‰) of this study. Furthermore, Hg concentrations in crop leaves (wheat: 12−45 μg/kg; corn: 9−24 μg/kg) in the NCP were relatively low (Rao and Wang 1987; Niu et al. 2011; Liu et al. 2012) and mostly been harvested. Hence, crop litter would not contribute significantly to the positive shifting of δ^{202}Hg in soils. We thus concluded that the positive shifting in δ^{202}Hg signals in soil Hg profile was mostly caused by the CFPP emissions through atmospheric deposition of GOM and PBM.

Conclusions

This study revealed that Hg emissions from a large CFPP operated for four decades in North China have a slight effect on the elevation of ambient GEM (<10 ng/m^3) and agricultural soil total Hg (<40 μg/kg). Although this CFPP historically emitted 17.5 tonnes of Hg into the surrounding atmosphere, only 3.9% of Hg was retained in the local soils due to the high proportion (79%) of GEM in the stack gas and the potential soil reemissions. Mercury isotopic signatures (δ^{202}Hg) revealed that THg increase in surface soil might be mainly caused by the

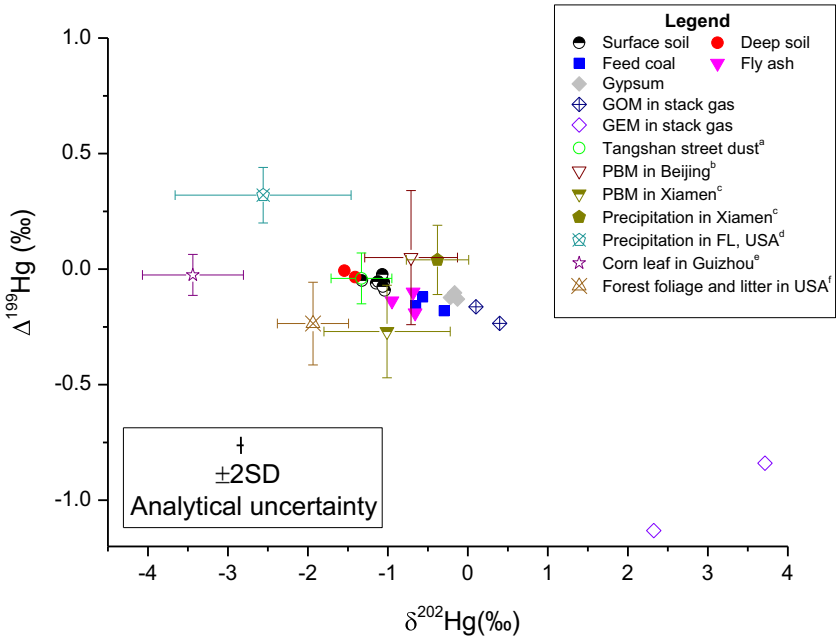

Fig. 4 Hg isotopic signatures in agricultural soil, feed coal, fly ash, gypsum, and stack gas of this study and other environmental media reported in literatures (the error bar stands for 1 SD. (a) Sun et al. (2020), (b) Huang et al. (2016), (c) Huang et al. (2018), (d) Sherman et al. (2012), (e) Sun et al. (2019a), (f) Zheng et al. (2016)

local CFPP emissions. Future studies should quantify the local dry/wet Hg deposition and reemission from the soil-air surface, as well as investigating CFPPs with varying Hg speciation in stack gas in order to obtain a more complete knowledge of the Hg biochemistry in the environment affected by CFPPs.

Supplementary Information The online version contains supplementary material available at https://doi.org/10.1007/s11356-021-12842-9

Acknowledgements The authors would thank Zhuo Lu and Xu Yang for their kindly help during the field sampling, and Xinyu Li for the visualization. Constructive comments from the two anonymous reviewers are also greatly acknowledged.

Author contribution Conceptualization: Zhonggen Li, Taishan Li, Xinbin Feng; Data curation: Zhonggen Li; Formal analysis: Zhonggen Li; Funding acquisition: Zhonggen Li, Taishan Li; Investigation: Zhonggen Li, Xufeng Chen, Wenli Liu, Taishan Li, Guangle Qiu, Guangyi Sun; Methodology: Haiyu Yan, Mingmeng Wang, Ji Chen, Qingfeng Wang; Project administration: Zhonggen Li, Taishan Li; Resources: Zhonggen Li, Xinbin Feng; Software: Zhonggen Li; Writing – original draft: Zhonggen Li; Writing – review & editing: Zhonggen Li, Qingfeng Wang.

Funding This work is financially supported by the Science & Technology Research and Development Plan of Tangshan (No. 12130215A), the Natural Science Foundation of China (No. 41967044), the Science and Technology Project of Guizhou Provincial Science and Technology Department (No. Qian-Ke-He-Ping-Tai-Ren-Cai [2017]5727-07), and the Doctoral Foundation Project of Zunyi Normal College (No. Zun-Shi BS [2018]15).

Data availability All data generated or analyzed during this study are included in this published article and its supplementary information files.

Declarations

Ethics approval Not applicable.

Consent to participate Not applicable.

Consent for publication Not applicable.

Competing interests The authors declare no competing interests.

References

AMAP/UNEP (2008) (Arctic Monitoring and Assessment Programme/United Nations Environment Programme). Technical background report to the global atmospheric mercury assessment. AMAP/UNEP Chemicals Branch, Nairobi

Antonio J, Martín R, Nanos N (2016) Soil as an archive of coal-fired power plant mercury deposition. J Hazard Mater 308:131–138

Blum JD, Bergquist BA (2007) Reporting of variations in the natural isotopic composition of mercury. Anal Bioanal Chem 388:353–359

Chen JS, Luo JJ, Luo JY (2009) Study on the mercury emission from seawater for coal-fired flue gas de-sulphurization during aeration process. Proc CSEE (Zhongguodianjixuebao) 29(11):39–43 (In Chinese with English Abstract)

Cheng Z, Tang Y, Li E, Wu Q, Wang L, Liu K, Wang S, Huang Y, Duan L (2020) Mercury accumulation in soil from atmospheric deposition in temperate steppe of Inner Mongolia, China. Environ Pollut 258:113692

Crockett AB, Kinnison RR (1979) Mercury residues in soil around a large coal-fired power plant. Environ Sci Technol 13:712–715

Cui L, Feng X, Lin CJ, Wang X, Meng B, Wang X, Wang H (2014) Accumulation and translocation of 198Hg in four crop species. Environ Toxicol Chem 33:334–340

Cui X, Wang X, Liu B (2020) The characteristics of heavy metal pollution in surface dust in Tangshan, a heavily industrialized city in North China, and an assessment of associated health risks. J Geochem Explor 210:106432

Dai S, Finkelman RB (2018) Coal geology in China: an overview. Int Geol Rev 60:531–534

Driscoll CT, Mason RP, Chan HM, Jacob DJ, Nicola P (2013) Mercury as a global pollutant: sources, pathways, and effects. Environ Sci Technol 47:4967–4983

Dutt U, Nelson PF, Morrison AL, Strezov V (2009) Mercury wet deposition and coal-fired power station contributions: an Australian study. Fuel Process Technol 90:1354–1359

Ebinghaus R, Kock HH, Coggins AM, Spain TG, Jennings SG, Temme C (2002) Long-term measurements of atmospheric mercury at Mace Head, Irish west coast, between 1995 and 2001. Atmos Environ 36:5267–5276

Eckley CS, Blanchard P, Mc Lennan D, Mintz R, Sekela M (2015) Soil −air mercury flux near a large industrial emission source before and after closure (Flin Flon, Manitoba, Canada). Environ Sci Technol 49:9750–9757

Edgerton ES, Hartsell BE, Jansen JJ (2006) Mercury speciation in coal-fired power plant plumes observed at three surface sites in the southeastern U.S. Environ. Sci.Technol 40:4563–4570

Fu XW, Feng X, Shang LH, Wang SF, Zhang H (2012) Two years of measurements of atmospheric total gaseous mercury (TGM) at a remote site in Mt. Changbai area, Northeastern China. Atmos Chem Phys 12:4215–4226

Gao Y, Wang Z, Zhang X, Wang C (2020) Observation and estimation of mercury exchange fluxes from soil under different crop cultivars and planting densities in North China Plain. Environ Pollut 259:113833

GB 15618-2018 (2018) Risk control standard for soil contamination of agricultural land in soil environmental quality, issued by MEE (Ministry of Ecology and Environment of the People's Republic of China). China Environment press, Beijing (in Chinese)

GB 3095–2012 (2012) Ambient Air Quality Standard. Issued by MEP (Ministry of Environmental Protection of the People's Republic of China). China Environment press, Beijing (in Chinese)

Gratz LE, Eckley CS, Schwantes SJ, Mattson E (2019) Ambient mercury observations near a coal-fired power plant in a western U.S. urban area. Atmosphere 10:176

Gustin MS, Bank MS, Bishop K, Bowman K, Branfireun B, Chételat J, Eckley CS, Hammerschmidt CR, Lamborg C, Lyman S, Martínez-Cortizas A, Sommar J, Tsui MT-K, Zhang T (2020) Mercury biogeochemical cycling: a synthesis of recent scientific advances. Sci Total Environ 737:139619

Gutiérrez-Mosquera H, Sujitha SB, Jonathan MP, Sarkar SK, Medina-Mosquera F, Ayala-Mosquera H, Morales-Mira G, Arreola-Mendoza L (2018) Mercury levels in human population from a mining district in Western Colombia. J Environ Sci 68:83–90

Gworek B, Dmuchowski W, Baczewska AH, Bragoszewska P, Bemowska-Kalabun O, Wrzosek-Jakubowska J (2017) Air contamination by mercury, emissions and transformations-a review. Water Air Soil Pollut 228:123

Huang Q, Chen J, Huang W, Fu P, Guinot B, Feng X, Shang L, Wang Z, Wang Z, Yuan S, Cai H, Wei L, Yu B (2016) Isotopic composition

for source identification of mercury in atmospheric fine particles. Atmos Chem Phys 16:11773–11786

Huang S, Sun L, Zhou T, Yuan D, Du B, Sun X (2018) Natural stable isotopic compositions of mercury in aerosols and wet precipitations around a coal-fired power plant in Xiamen, southeast China. Atmos Environ 173:72–80

Jackson TA, Muir DCG (2012) Mass-dependent and mass-independent variations in the isotope composition of mercury in a sediment core from a lake polluted by emissions from the combustion of coal. Sci Total Environ 417-418:189–203

Jiang L (2006) The heavy metal concentrations and soil quality evaluation in the Fengrun region, Tangshan city, Heibei province. In: Master thesis of China University of Geosciences (Beijing) (in Chinese with English abstract)

Jiang P, Chen Z, Lu X, Tu Z, Wang Z (2007) An investigation of atmospheric Hg concentration and the removal of Hg by desulfurizing in flue gas of coal fired power plants in Guizhou area. Chin J Environ Eng(Huanjinggongchengxuebao) 1:80–83 (in Chinese with English abstract)

Kalinchuk VV, Mishukov VF, Astakhov AS (2018) Arctic source for elevated atmospheric mercury (Hg0) in the western Bering Sea in the summer of 2013. J Environ Sci 68:114–121

Keeler GJ, Landis MS, Norris GA, Christianson EM, Dvonch JT (2006) Sources of mercury wet deposition in Eastern Ohio, USA. Environ Sci Technol 40(19):5874–5881

Li P, Feng X, Qiu G, Li Z, Fu X, Sakamoto M, Liu X, Wang D (2008) Mercury exposures and symptoms in smelting workers of artisanal mercury mines in Wuchuan, Guizhou, China. Environ Res 107: 108–114

Li R, Wu H, Ding J, Fu W, Gan L, Li Y (2017) Mercury pollution in vegetables, grains and soils from areas surrounding coal-fired power plants. Sci Rep 7:46545

Li Z, Chen X, Liu W, Li T, Chen J, Lin C-J, Sun G, Feng X (2019) Evolution of four-decade atmospheric mercury release from a coal-fired power plant in North China. Atmos Environ 213:526–533

Lindqvist O, Johansson K, Aastrup M, Andersson A, Bringmark L, Hovsenius G, Håkanson L, Iverfeldt Å, Mieli M, Timm B (1991) Mercury in the Swedish environment. Recent research on causes, consequences and corrective methods. Water Air Soil Pollut 56:1–261

Liu K, Wu Q, Wang L, Wang S, Liu T, Ding D, Tang Y, Li G, Tian H, Duan L, Wang X, Fu X, Feng X, Hao J (2019) Measure-specific effectiveness of air pollution control on China's atmospheric mercury concentration and deposition during 2013–2017. Environ Sci Technol 53:8938–8946

Liu W, Li B, Wu M, Li Y (2012) The influence of coal-fired flue gas on accumulation and distribution and distribution of mercury in soil–wheat system. J Agro-Environ Sci (Nongyehuanjingkexuexuebao) 31:30–35 (in Chinese with English abstract)

Lohman K, Seigneur C, Edgerton E, Jansen J (2006) Modeling mercury in power plant plumes. Environ Sci Technol 40:3848–3854

Lu J, Cheng J, Hu X, Xie H, Wang W (2006) The research of mercury-polluted soil and leaves around Shanghai Wujing industrial zone. Environ Chem (Huanjinghuaxue) 25:101–103 (in Chinese with English abstract)

Martin JAR, Nanos N, Grigoratos T, Carbonell G, Samara C (2014) Local deposition of mercury in topsoils around coal-fired power plants: is it always true? Environ Sci Pollut Res 21:10205–10214

Mason RP, Fitzgerald WF, Morel FMM (1994) The Biogeochemical cycling of elemental mercury: anthropogenic influence. Geochim Cosmochim Ac 58:3191–3198

Mazur M, Mintz R, Lapalme M, Wiens B (2009) Ambient air total gaseous mercury concentrations in the vicinity of coal-fired power plants in Alberta, Canada. Sci Total Environ 408:373–381

Mou S, Tang S (1992) An investigation into the mercury pollution of a soil-vegetable system in an acid precipitation area. Agro-environ Prot (Nongyehuanjingbaohu) 11:57–60 (in Chinese with English abstract)

Navrátil T, Shanley JB, Rohovec J, Oulehle F, Simecek M, Houska J, Cudlín P (2016) Soil mercury distribution in adjacent coniferous and deciduous stands highly impacted by acid rain in the Ore Mountains, Czech Republic. Appl Geochem 75:63–75

Niu Z, Zhang X, Wang Z, Ci Z (2011) Field controlled experiments of mercury accumulation in crops from air and soil. Environ Pollut 159:2684–2689

NY/T 1121.6-2006 (2006). Soil testing, Part 6: Method for determination of soil organic matter. Standard method issued by Ministry of Agriculture of China, Beijing. (in Chinese)

NY/T 1377-2007 (2007). Determination of pH in soil. Standard method issued by Ministry of Agriculture of China, Beijing. (in Chinese)

O'Connor D, Hou D, Ok YS, Mulder J, Duan L, Wu Q, Wang S, Tack FMG, Rinklebe J (2019) Mercury speciation, transformation, and transportation in soils, atmospheric flux, and implications for risk management: a critical review. Environ Int 126:747–761

Okedeyi OO, Dube S, Awofolu OR, Nindi MM (2014) Assessing the enrichment of heavy metals in surface soil and plant (Digitaria eriantha) around coal-fired power plants in South Africa. Environ Sci Pollut Res 21:4686–4696

Pacyna EG, Pacyna JM (2002) Global emission of mercury from anthropogenic sources in 1995. Water Air Soil Pollut 137:149–165

Pérez PA, Hintelmann H, Lobos G, Bravo MA (2019) Mercury and methylmercury levels in soils associated with coal-fired power plants in central-northern Chile. Chemosphere 237:124535

Rao L, Wang J (1987) Mercury content of some crops and industrial crops in the North China Plain. Acta Ecologica Sinica (Shengtaixuebao) 7(3):287–288 (In Chinese)

Rydberg J, Klaminder R, Rosen R, Bindler R (2010) Climate driven release of carbon and mercury from permafrost mires increases mercury loading to Sub-Arctic Lakes. Sci Total Environ 408(20):4778–4783

Seigneur C, Vijayaraghavan K, Lohman K (2006) Atmospheric mercury chemistry: Sensitivity of global model simulations to chemical reactions. J Geophys Res 111:D22306

Sherman LS, Blum JD, Keeler GJ, Demers JD, Dvonch JT (2012) Investigation of local mercury deposition from a coal-fired power plant using mercury isotopes. Environ Sci Technol 46:382–390

Sommar J, Zhu W, Shang L, Lin C-J, Feng X (2016) Seasonal variations in metallic mercury (Hg0) vapor exchange over biannual wheat-corn rotation cropland in the North China Plain. Biogeosciences 13: 2029–2049

Streets DG, Devane MK, Lu Z, Bond TC, Sunderland EM, Jacob DJ (2011) All-time releases of mercury to the atmosphere from human activities. Environ Sci Technol 45:10485–10491

Streets DG, Hao J, Wu Y, Jiang J, Chan M, Tian H, Feng X (2005) Anthropogenic mercury emissions in China. Atmos Environ 39: 7789–7806

Streets DG, Lu Z, Levin L, ter Schure AFH, Sunderland EM (2018) Historical releases of mercury to air, land, and water from coal combustion. Sci Total Environ 615:131–140

Sullivan, T. M.; Bowerman, B.; Adams, J.; Milian, L.; Lipfert, F.; Subramaniam, S.; Blake, R. (2005) Local impacts of mercury emissions from coal fired power plants. Report of Brookhaven National Laboratory, Upton, NY, Presented at Air Quality V Washington, D.C. September 21–23. https://www.researchgate.net/publication/228627955_Local_impacts_of_mercury_emissions_from_coal_fired_power_plants, .

Sun R (2019) Mercury stable isotope fractionation during coal combustion in coal-fired boilers: reconciling atmospheric Hg isotope observations with Hg isotope fractionation theory. Bull Environ Contam Toxicol 10:657–664

Sun G, Feng X, Yang C, Zhang L, Yin R, Li Z, Bi X, Wu Y (2020) Levels, sources, isotope signatures, and health risks of mercury in street dust across China. J Hazard Mater 392:122276

Sun G, Feng X, Yin R, Zhao H, Zhang L, Sommar J, Li Z, Zhang H (2019a) Corn (Zea mays L.): A low methylmercury staple cereal source and an important biospheric sink of atmospheric mercury, and health risk assessment. Environ Int 131:104971

Sun L, Guo D, Liu K, Meng H, Zheng Y, Yuan F, Zhu G (2019b) Levels, sources, and spatial distribution of heavy metals in soils from a typical coal industrial city of Tangshan, China. Catena 175:101–109

Sun R, Enrico M, Heimburger LE, Scott C, Sonke JE (2013) A double-stage tube furnace-acid-trapping protocol for the pre-concentration of mercury from solid samples for isotopic analysis. Anal Bioanal Chem 405:6771–6781

Sun R, Streets DG, Horowitz HM, Amos HM, Liu G, Perrot V, Toutain J-P, Hintelmann H, Sunderland EM (2016) Historical (1850–2010) mercury stable isotope inventory from anthropogenic sources to the atmosphere. Elementa Sci Anthrop 4:000091

Tang Q, Liu G, Zhou C, Zhang H, Sun R (2013) Distribution of environmentally sensitive elements in residential soils near a coal-fired power plant: potential risks to ecology and children's health. Chemosphere 93:2473–2479

Tang S, Feng C, Feng X, Zhu J, Sun R, Fan H, Wang L, Li R, Mao T, Zhou T (2017) Stable isotope composition of mercury forms in flue gases from a typical coal-fired power plant, Inner Mongolia, northern China. J Hazard Mater 328:90–97

Tang S, Feng X, Qiu J, Yin G, Yang Z (2007) Mercury speciation and emissions from coal combustion in Guiyang, southwest China. Environ Res 105(2):175–182

UNEP (United Nations Environment Programme) (2019). Global Mercury Assessment 2018. UNEP Chemicals and Health Branch Geneva, Switzerland. http://wedocs.unep.org/bitstream/handle/20.500.11822/27579/GMA2018.pdf?sequence=1&isAllowed=y, .

UNEP (United Nations Environment Programme) (2002). Global mercury assessment. Geneva, Switzerland.

U.S. EPA(United States Environmental Protection Agency) (1997). Mercury study report to congress. Volume I: Executive Summary. United States Environmental Protection Agency EPA-452/R-97-003, Office of Air Quality Planning and Standards & Office of Research and Development, NC. https://www.epa.gov/mercury/mercury-study-report-congress , .

Wang J, Wang W, Xu W, Wang X, Zhao S (2011a) Mercury removals by existing pollutants control devices of four coal-fired power plants in China. J Environ Sci 23:1839–1844

Wang, J.; Wang, X.; Xu, M.; Zhang, W. (2013a) Soil organic carbon dynamics in wheat-maize cropping systems of north China: application of isotope approach to long-term experiments. AGU Fall Meeting Abstracts, December 2013. https://ui.adsabs.harvard.edu/abs/2013AGUFM.B23C0566W/abstract. .

Wang Q, Shen W, Ma Z (2000) Estimation of mercury emission from coal combustion in China. Environ Sci Technol 34:2711–2713

Wang Q, Zhang J, Xin X, Zhao B, Ma D, Zhang H (2016) The accumulation and transfer of arsenic and mercury in the soil under a long-term fertilization treatment. J Soils Sediments 16:427–437

Wang XH, Wang J, Wang WH (2011b) Effects of flue gas mercury emission from two coal-fired power plants in Shanghai on peripheral environment. Chin J Ecol(Shengtaixuezazhi) 30:928–932 (in Chinese with English abstract)

Wang Y, Huang J, Hopke PK, Rattigan OV, Chalupa DC, Utell MJ, Holsen TM (2013b) Effect of the shutdown of a large coal-fired power plant on ambient mercury species. Chemosphere 92:360–367

Wiederhold JG, Smith RS, Siebner H, Jew AD, Brown GE, Bourdon B, Kretzschmar R (2013) Mercury isotope signatures as tracers for hg cycling at the New Idria Hg mine. Environ Sci Technol 47(12):6137–6145

Wright LP, Zhang L, Cheng I, Aherne J, Wentworth GR (2018) Impacts and effects indicators of atmospheric deposition of major pollutants to various ecosystems—a review. Aerosol Air Qual Res 18:1953–1992

Wu Q, Wang S, Wang L, Liu F, Lin C-J, Zhang L, Wang F (2014) Spatial distribution and accumulation of Hg in soil surrounding a Zn/Pb smelter. Sci Total Environ 496:668–677

Xu J, Kleja DB, Biester H, Lagerkvist A, Kumpiene J (2014) Influence of particle size distribution, organic carbon, pH and chlorides on washing of mercury contaminated soil. Chemosphere 109:99–105

Xu X, Meng B, Zhang C, Feng X, Gu C, Guo J, Bishop K, Xu Z, Zhang S, Qiu G (2017) The local impact of a coal-fired power plant on inorganic mercury and methyl-mercury distribution in rice (Oryza sativa L.). Environ Pollut 223:11–18

Yang A, Wang Q, Wu W, Yuan X (2012) Investigation on mercury pollution in surrounding environment of a coal-fired power plant in Guizhou. J Henan Agric Sci (Henannongyekexue) 41:69–73 (in Chinese with English abstract)

Yang X, Wang L (2008) Spatial analysis and hazard assessment of mercury in soil around the coal-fired power plant: a case study from the city of Baoji, China. Environ Geol 53:1381–1388

Yin R, Feng X, Foucher D, Shi W, Zhao Z, Wang J (2010) High precision determination of mercury isotope ratios using online mercury vapor generation system coupled with multicollector inductively coupled plasma-mass spectrometer. Chin J Anal Chem 38:929–934

Yin R, Feng X, Wang J, Bao Z, Yu B, Chen J (2013) Mercury isotope variations between bioavailable mercury fractions and total mercury in mercury contaminated soil in Wanshan Mercury Mine, SW China. Chem Geol 336:80–86

Yin R, Feng X, Hurley JP, Krabbenhoft DP, Lepak RF, Hu R, Zhang Q, Li Z, Bi X (2016) Mercury isotopes as proxies to identify sources and environmental impacts of mercury in sphalerites. Sci Rep 6:18686

Zhang L, Wang SX, Wang L, Hao JM (2013) Atmospheric mercury concentration and chemical speciation at a rural site in Beijing, China: implications of mercury emission sources. Atmos Chem Phys 13:10505–10516

Zhang L, Wang S, Wang L, Wu Y, Duan L, Wu Q, Wang F, Yang M, Yang H, Hao J, Liu X (2015) Updated emission inventories for speciated atmospheric mercury from anthropogenic sources in China. Environ Sci Technol 48:3575–3582

Zhang, Y. 2017. The study of heavy metal pollution characteristics in soil of Fengnan region, Tangshan city. Master thesis of Hebei University of Science and Technology. (In Chinese with English Abstract).

Zhang Y, Jaeglé L (2013) Decreases in mercury wet deposition over the United States during 2004–2010: roles of domestic and global background emission reductions. Atmosphere 4:113–131

Zheng J, Zhou J, He S, Luo Z (2009) Environmental impact of mercury emission from a coal-fired power plant. CIESC J (Huagongxuebao) 60:3104–3111 (in Chinese with English abstract)

Zheng R, Liu Q, Wu W (2015) The construction history of Douhe power plant—a result of Four-Three Plan. Energy (Nengyuan) 8:108–112 (in Chinese)

Zheng W, Obris D, Weis D, Bergquist BA (2016) Mercury isotope compositions across North American forests. Global Biogeochem Cy 30:1475–1492

Zhu W, Li ZG, Li P, Yu B, Lin C-J, Sommar J, Feng XB (2018) Re-emission of legacy mercury from soil adjacent to closed point sources of Hg emission. Environ Pollut 242:718–727